Molecular Therapy
Oncolytics
Original Article

lncRNA DSCR8 mediates miR-137/Cdc42 to regulate gastric cancer cell proliferation, invasion, and cell cycle as a competitive endogenous RNA

Zhengwei Chen,[1] Chaobo Xu,[1] Xiaoming Pan,[1] Guoxiong Cheng,[1] Ming Liu,[1] Jiaxin Li,[1] and Yijun Mei[1]

[1]Department of Gastrointestinal Surgery, Lishui People's Hospital of Zhejiang Province, 15 Dazhong Street, Liandu District, Lishui City, Zhejiang 323000, China

lncRNA DSCR8 (Down syndrome critical region 8) is involved in progression of many cancers, but its specific role in gastric cancer (GC) is still unclear. Here, qRT-PCR detected upregulated expression of DSCR8 and Cdc42 and downregulated expression of miR-137 in GC. The protein expression level of Cdc42 in GC was upregulated as tested by western blot. Statistical analysis showed that DSCR8 was closely associated with some malignant clinicopathological features (such as tumor size, metastasis, and stage) in GC patients. Fluorescence *in situ* hybridization showed that DSCR8 was localized in the nucleus and cytoplasm. Dual-luciferase reporter gene, RNA immunoprecipitation, and biotin pull-down assays showed that DSCR8 could bind to miR-137 could bind to Cdc42. *In vitro* and *in vivo* assays showed that DSCR8 could promote proliferation, invasion, and the cycle of GC cells and inhibit cell apoptosis. In addition, a rescue experiment showed that DSCR8 regulated progression of GC cells via miR-137. Furthermore, DSCR8 regulated Cdc42 in GC cells by inhibiting miR-137. Taken together, these data indicated that DSCR8 could adsorb miR-137 to reduce its inhibitory effect on Cdc42 expression, thereby promoting the progression of GC cells and regulating the cell cycle. These results provide a novel direction for DSCR8 as a target of GC.

INTRODUCTION

Gastric cancer (GC) is the fourth most frequent malignancy and the second leading cause of cancer deaths.[1] Surgical treatment for patients with early diagnosis of GC leads to a good prognosis, but most GC patients lose the opportunity of surgery as they are diagnosed in the middle and late stage. At present, most patients with advanced GC receive radiotherapy and chemotherapy,[2] although adverse reactions caused by chemotherapy will seriously reduce the quality of life of the patients, which is not conducive to the prognosis of the patients.[3,4] Therefore, it is an urgent problem to seek new treatment regimens to improve the therapeutic efficacy and survival rate of patients with gastric cancer. Targeted therapy for patients with malignant tumors is the current hotspot of tumor treatment, and molecular targeted drug therapy for patients with GC has made some progress.[5,6] Further understanding the molecular mechanism of GC progression and metastasis and exploring effective biomarkers are of great importance for the diagnosis and novel treatment of GC patients.

Long non-coding RNAs (lncRNAs) are non-coding transcripts more than 200 nt long without potential protein coding capacity.[1] A growing number of studies show that lncRNAs are involved in a variety of biological processes, including chromatin interaction, transcriptional regulation, mRNA posttranscriptional regulation, and epigenetic regulation.[7–9] The regulation of lncRNA expression is more refined, and the cell- or tissue-specific aspect of lncRNA expression is higher than that of mRNA.[10] The expression levels of most lncRNAs are extremely low in normal times, but they are upregulated under pathological conditions. A large number of lncRNAs are expressed in this pattern in different tissues, especially in specific types of tumors.[11,12] Therefore, the determination of lncRNA can trace the metastasis of tumor or the origin of tumor cells in the circulatory system. Due to cell- and tissue-specific factors, lncRNAs become excellent biomarkers for biological events such as disease treatment.[13] Recently, a novel regulatory mechanism has been discovered that involves crosstalk between lncRNAs and mRNAs by competing for shared microRNA (miRNA) response elements. In this case, lncRNAs may act as competitive endogenous RNAs (ceRNAs) to sponge miRNAs, thereby regulating the disinhibition of miRNA targets and increasing the expression level of target genes.[14] New evidence also indicates that lncRNA is a key regulatory factor in the occurrence and development of GC. For example, lncRNA MEG3 inhibits GC cell proliferation and metastasis via the p53 signaling pathway.[15] Highly expressed lncRNA p4516 can serve as a marker for the prognosis of GC patients.[16] lncRNA NORAD promotes GC proliferation and inhibits apoptosis by modulating the miR-214/Akt/mTOR axis.[17] Therefore, it is of great significance to study lncRNAs for the purpose of learning more about the molecular regulatory mechanisms in the progression of cancers.

lncRNA DSCR8 (Down syndrome critical region 8), also known as MMA-1, is located on chromosome 21q22.13. Studies have found that MMA-1a and MMA-1b are new members of the cancer/testis

Received 7 December 2020; accepted 19 May 2021;
https://doi.org/10.1016/j.omto.2021.05.010.

Correspondence: Yijun Mei, Department of Gastrointestinal Surgery, Lishui People's Hospital of Zhejiang Province, 15 Dazhong Street, Liandu District, Lishui City, Zhejiang 323000, China.
E-mail: meiyijunyi@163.com

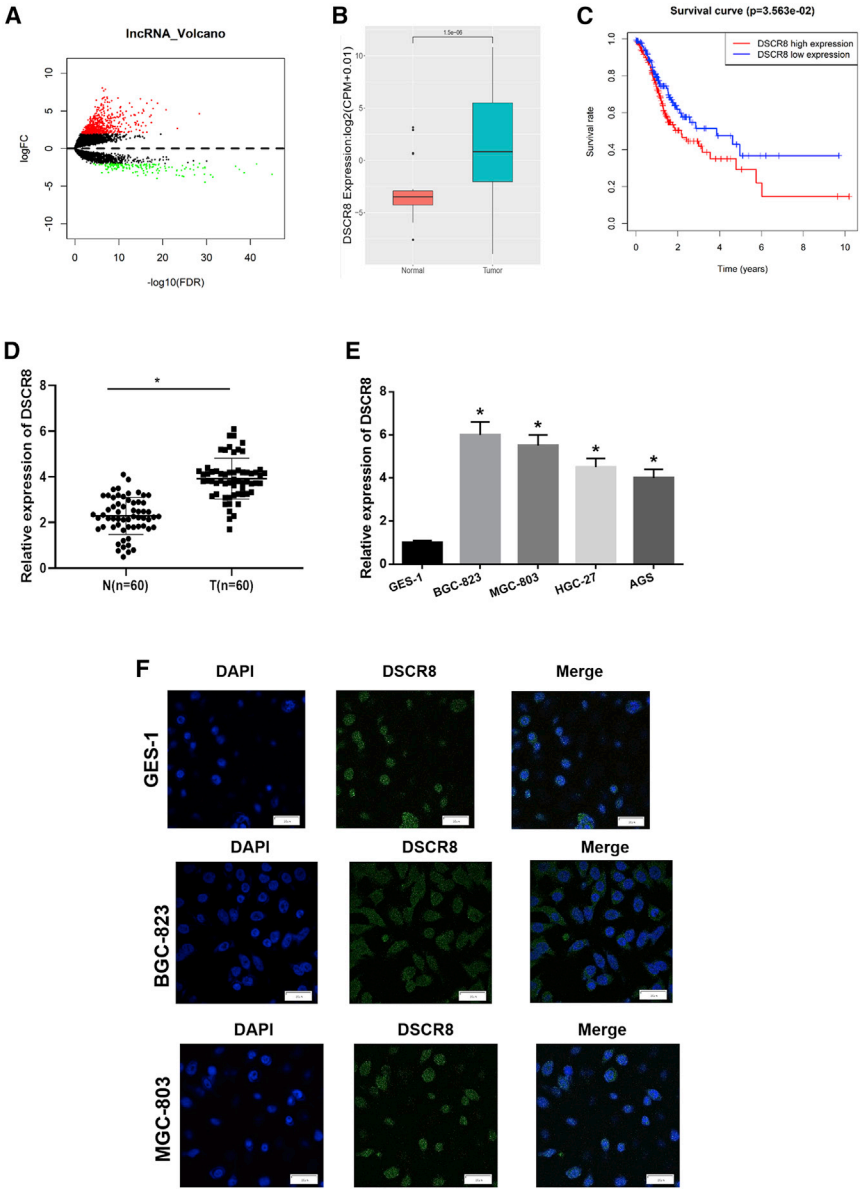

Figure 1. lncRNA DSCR8 is upregulated in GC and is associated with poor survival

(A) Volcano plot of DElncRNAs. (B) Differential expression of DSCR8 in TCGA-STAD dataset. (C) Survival curves of patients with high and low DSCR8 expression. (D and E) Expression of DSCR8 in (D) GC tissue samples and adjacent normal tissue samples as well as in (E) human normal stomach cell line GES-1 and human GC cell lines BGC-823, MGC-803, HGC-27, and AGS. (F) Localization of DSCR8 in BGC-823 and MGC-803 cell lines (Scale, 20 μm). All data are measured data, expressed as mean ± standard deviation. n = three independent experiments. *p < 0.05.

antigen family, and they are both highly expressed in uterine cancer and melanoma.[18,19] However, the expression and function of DSCR8 in GC remain largely unknown. miR-137 plays a role in various cancers as an anti-cancer factor. For instance, miR-137 inhibits the proliferation and growth of non-small cell lung cancer (NSCLC)[20,21] and reduces the stemness of pancreatic cancer cells by targeting the KLF12-related Wnt/β-catenin pathway,[22] whereas silencing miR-137 can induce resistance of prostate cancer cells to bicalutamide by targeting TRIM24.[23] Moreover, research has identified that miR-137 expression is decreased in GC and negatively regulates Cdc42.[24] Cdc42 is a small GTPase that belongs to the subfamily of rho. Studies have elucidated that Cdc42 is closely related to the occurrence and development of cancers.[25,26] However, the mechanism of DSCR8 in the regulation of miR-137/Cdc42 remains to be fully elucidated.

In the present study, we investigated the expression, function, and mechanism of DSCR8 in GC cells, and we analyzed the targeted relationship between DSCR8 and miR-137. Our study provides a theoretical basis for understanding the mechanism by which DSCR8 regulates the progression of GC by the miR-137/Cdc42 axis and helps to explore a new direction for future diagnosis and treatment of GC.

RESULTS

lncRNA DSCR8 is significantly upregulated in GC tissue and cells

The relevant gene expression data were obtained from The Cancer Genome Atlas (TCGA)-STAD dataset. ID conversion was done by a gene transfer format (GTF) (GRCh38.p5) file, and then lncRNA expression profiles (including 32 normal tissue samples and 373 GC tissue samples) were extracted. The edgeR package of R language was used for differential analysis with the threshold set as |log fold change (FC)| >2, an adjusted (adj,) p value <0.05, and normal samples taken as control. In total, 769 differentially expressed lncRNAs (DElncRNAs) were obtained. Among them, 155 lncRNAs were differentially downregulated, while 614 lncRNAs were differentially upregulated (Figure 1A), of which DSCR8 was significantly upregulated in tumor tissue samples (Figure 1B). Among the 614 differentially upregulated lncRNAs, 99 were associated with prognosis. An increasing number of studies indicate that lncRNA DSCR8 may be involved in the progression of liver cancer, ovarian cancer, and other cancers.[27,28] Thus, DSCR8 plays an important role in the development of cancer, and we selected DSCR8 as the study object. In this study, samples were divided into a high-expression group and a low-expression group according to the median expression of DSCR8. Survival analysis was conducted using the "Survival" package, and the results indicated that DSCR8 showed a significant prognostic difference in patients, which meant that high

Table 1. Relationship between DSCR8 expression and clinicopathological features in GC

Characteristics		Cases (n = 60)	No. of patients		p
			DSCR8 (high)	DSCR8 (low)	
Sex	female	21	8	13	0.176
	male	39	22	17	
Age	<60	20	9	12	0.417
	≥60	40	21	18	
Tumor size (cm)	<5	28	12	16	0.038*
	≥5	32	18	14	
Metastasis	no	25	7	18	0.0040*
	yes	35	23	12	
Histologic type	diffuse	50	28	22	0.038
	intestinal	10	2	8	
Stage	I & II	30	8	22	< 0.001*
	III & IV	30	22	8	

*p < 0.05.

expression of DSCR8 was associated with significant poor prognosis (Figure 1C). In order to further verify the differential expression of DSCR8 in GC, qRT-PCR was performed to assess the expression of DSCR8 in clinical tissue samples, which showed that the expression of DSCR8 was remarkably high in GC tissue samples (Figure 1D). The general information of the samples is shown in Table 1. DSCR8 expression in GC tissue samples was found to be unrelated to sex, age, and histologic type, whereas it was considerably correlated with tumor size, metastasis, and stage.

In addition, four GC cell lines and one normal stomach cell line were subjected to qRT-PCR for detection of DSCR8 expression, and it was found that DSCR8 was markedly highly expressed in GC cell lines (Figure 1E), among which DSCR8 exhibited a relatively higher expression level in BGC-823 and MGC-803 cell lines. Additionally, the result of an RNA fluorescence *in situ* hybridization (FISH) experiment indicated that DSCR8 was localized in both the nucleus and cytoplasm (Figure 1F). Cytoplasmic expression is a necessary condition for ceRNA exerting its function. Therefore, BGC-823 and MGC-803 cell lines were selected for subsequent analysis.

Downregulation of DSCR8 inhibits GC cell proliferation, invasion, and the cell cycle and promotes cell apoptosis

To prove that DSCR8 is important in the progression of GC, short hairpin (sh-)DSCR8#1, sh-DSCR8#2, and sh-DSCR8#3 were first transfected into BGC-823 and MGC-803 cells to decrease DSCR8 expression, and qRT-PCR was conducted to evaluate transfection efficiency. The result showed that sh-DSCR8#2 (hereafter referred to as sh-DSCR8) had the most obvious inhibitory effect, so it was selected for subsequent experiments (Figure 2A). Subsequently, an MTT (3-(4,5-dimethylthiazol-2-yl)-2,5-diphenyltetrazolium bromide) assay was performed to determine the effect of DSCR8 on cell proliferation, which found that low DSCR8 expression inhibited GC cell proliferation ability (Figure 2B). In addition, a Transwell assay was carried out to measure cell invasion ability, while flow cytometry was performed to test the cell cycle. The results demonstrated that sh-DSCR8 decreased the invasion ability of GC cells (Figure 2C), and it promoted cell cycle progression, which was manifested as an increase in the number of cells in the G_0/G_1 phase (Figure 2D). Meanwhile, flow cytometry showed that DSCR8 silence had a promoting effect on tumor cell apoptosis (Figure 2E). Hence, we concluded that inhibition of DSCR8 could inhibit the progression of GC.

DSCR8 sponges miR-137 in GC cells

STAD miRNA expression data (45 normal tissue samples and 444 GC tissue samples) were downloaded from TCGA database. The edgeR package of R language was used to obtain 119 differentially expressed miRNAs (DEmiRNAs) with the threshold set as |logFC| >1.5, an adj. p value <0.05, and normal samples taken as control (Figure 3A). The miRcode database was applied for target prediction for DSCR8, and miR-137 and miR-205 were obtained from the intersection (Figure 3B) of predicted miRNAs and downregulated DEmiRNAs. Dong et al.[29] reported that upregulated miR-137 plays an anti-tumor role in GC cell lines. Therefore, miR-137 was selected as the object in this study (see Figure 3C for its targeted binding sites with DSCR8). qRT-PCR was performed on GC tissue samples (n = 60) and paired adjacent normal tissue samples (n = 60), which found that miR-137 was remarkably lowly expressed in GC tissue samples, consistent with miR-137 expression in samples obtained from TCGA database (Figure 3D). Pearson correlation analysis suggested that DSCR8 expression was negatively correlated with miR-137 expression in GC patients (Figure 3E). Additionally, miR-137 was found to be relatively lowly expressed in GC cell lines (Figure 3F).

Moreover, miR-137 was found to be negatively regulated by DSCR8 in GC cell lines transfected with plasmid cDNA3.1(pc-) DSCR8 (Figure 3G), while miR-137 was found to negatively affect DSCR8 expression in GC cell lines transfected with miR-137 mimic (Figure 3H). A dual-luciferase reporter gene assay demonstrated that miR-137 directly targeted the 3′ untranslated region (UTR) of wild-type (WT)-DSCR8 and negatively regulated the activity of luciferase of WT-DSCR8 3′ UTR (Figure 3I). An RNA immunoprecipitation (RIP) experiment showed that DSCR8 was enriched in the RNAs pulled down by Ago2 protein in the miR-137 mimic group (Figure 3J). In addition, the biotin-labeled pull-down assay showed that DSCR8 expression was significantly increased in the Bio-WT-miR-137 binding group compared to the Bio-negative control (NC) group (Figure 3K). Taken together, these findings illustrate that miR-137 is a downstream target of DSCR8 in GC cells.

miR-137 meditates the effect of DSCR8 on GC cell proliferation, invasion, the cell cycle, and cell apoptosis

To investigate whether miR-137 could interact with DSCR8 to affect GC cell proliferation, invasion, the cell cycle, and cell apoptosis, rescue

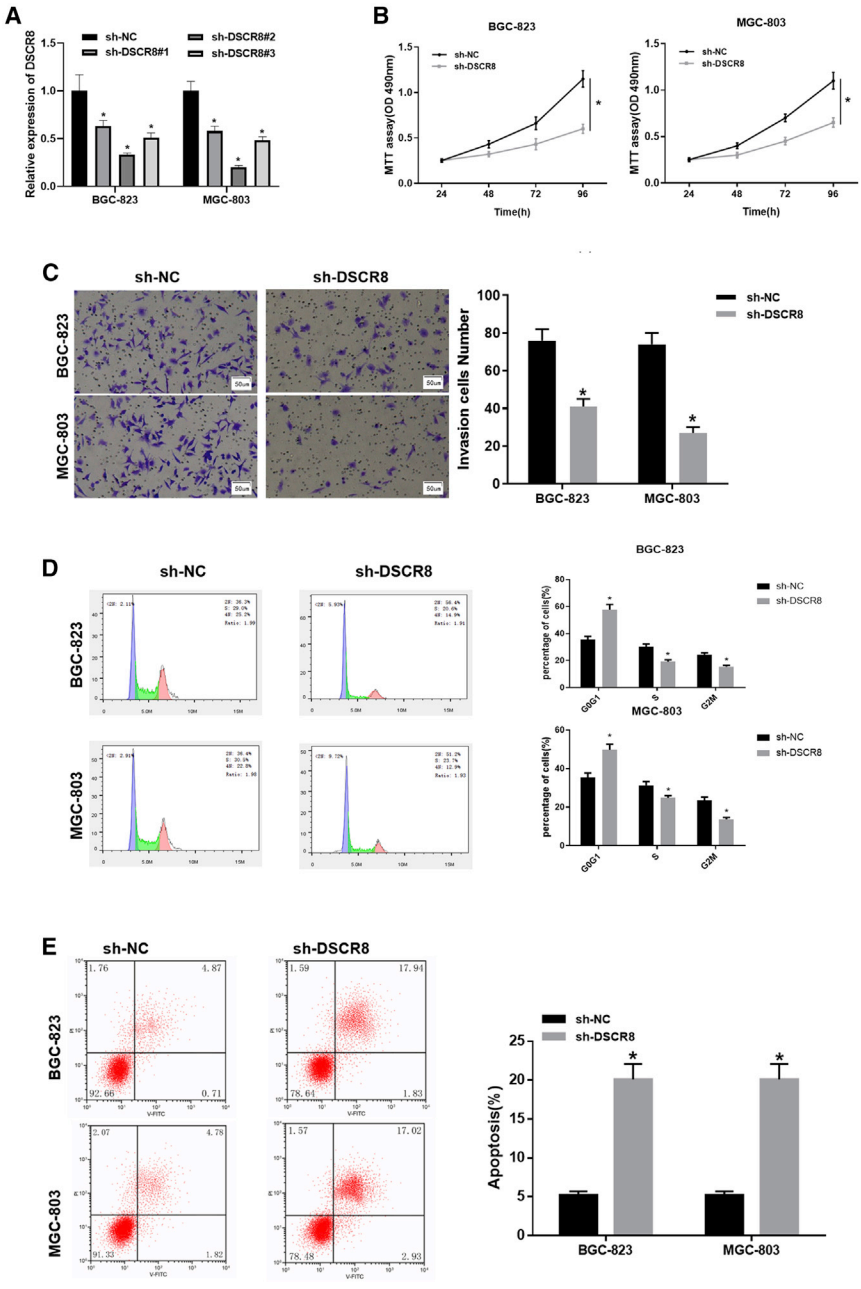

Figure 2. Downregulation of DSCR8 inhibits GC cell proliferation, invasion and cell cycle as well as promotes cell apoptosis

(A) DSCR8 expression level in transfected cells. (B) Proliferation of cells in each transfection group. (C) Invasion of cells in each transfection group (100×). (D) Cell cycle in each transfection group. (E) Apoptosis of cells in each transfection group. n = three independent experiments. All data are measured data, expressed as mean ± standard deviation. *p < 0.05.

experiments were performed. First, the expression levels of DSCR8 and miR-137 in each transfected group were detected by qRT-PCR. The results showed that DSCR8 was inhibited by miR-137 mimic (compared with the pc-NC+mimic NC group). Meanwhile, miR-137 was significantly downregulated after overexpression of DSCR8 (compared with the pc-NC+miR-137 mimic group) (Figure 4A). It was found that overexpressing miR-137 could inhibit GC cell proliferation (Figure 4B) and invasion (Figure 4C) abilities, as well as inhibit cell cycle progression, which was manifested as an increase in the number of cells in the G_0/G_1 phase (Figure 4D), and facilitate GC cell apoptosis (Figure 4E). In addition, we noticed that overexpressing miR-137 attenuated the promoting effect of DSCR8 on cell proliferation, invasion, and the cell cycle, and it reversed the inhibitory effect of DSCR8 on cell apoptosis. Therefore, these experiments proved that DSCR8 regulated GC cell proliferation, invasion, the cell cycle, and cell apoptosis by mediating miR-137.

DSCR8 regulates Cdc42 expression by suppressing miR-137 in GC cells

Previous studies have reported that miR-137 can target the expression of Cdc42 in GC,[24] lung cancer,[26] and intestinal cancer.[30] Therefore, Cdc42 was selected as the downstream target gene of miR-137 in our study. We found that miR-137 had binding sites with the 3′ UTR of Cdc42 mRNA by the TargetScan website (http://www.targetscan.org/vert_71/) (Figure 5A). Similarly, a dual-luciferase reporter gene assay and RIP experiment were performed to prove the binding relationship between miR-137 and Cdc42, the results of which indicated that the activity of luciferase of the WT-Cdc42 3′ UTR was markedly inhibited in GC cells transfected with miR-137 mimic, while that in GC cells co-transfected with the miR-137 mimic and pc-DSCR8 was significantly increased. The results illustrated that DSCR8 sponged miR-137 to reduce the binding between miR-137 and Cdc42 (Figure 5B). RIP experiments found that the RNAs pulled down by Ago2 protein were enriched in Cdc42 mRNA. In addition, the RIP experiments showed that overexpression of DSCR8 could restore the expression of Cdc42 mRNA in the Ago2 complex (Figure 5C). The expression level of Cdc42 in GES-1 and GC cells was detected by qRT-PCR. The results showed that Cdc42 in GC cell lines was upregulated compared with GES-1 cells (Figure 5D). Likewise, as revealed by qRT-PCR and western blot, Cdc42 exhibited a relatively higher expression level in GC tissue than that in normal tissue (Figures 5E and 5F), which was consistent with the result of TCGA database. Pearson correlation analysis indicated that miR-137 was negatively

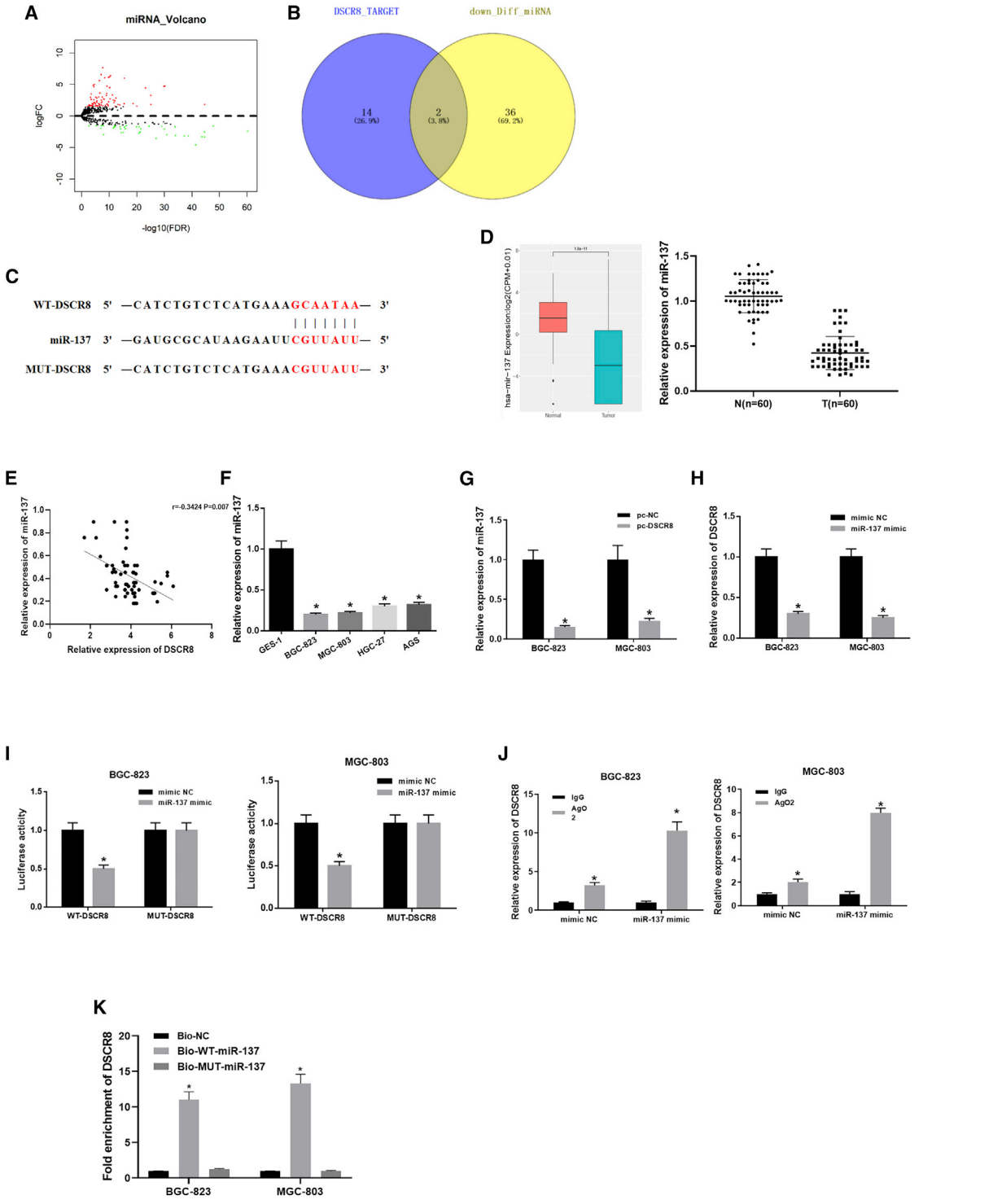

Figure 3. DSCR8 sponges miR-137 in GC cells

(A) Volcano plot of DEmiRNAs. (B) A Venn diagram was made to find the candidate genes from the intersection of target genes of DSCR8 predicted by the miRcode database and downregulated DEmiRNAs. (C) Binding sites of miR-137 on the DSCR8 3′ UTR. (D) Differential expression of miR-137 in GC tissue (left, TCGA-STAD samples; right,

(legend continued on next page)

correlated with Cdc42 in GC patients, while DSCR8 was positively correlated with Cdc42 (Figure 5G).

Furthermore, to validate whether DSCR8 could function on GC cells by affecting Cdc42, qRT-PCR and western blot were performed to determine Cdc42 expression in different groups, which found that compared with the sh-NC+overexpressed (oe-)NC group, silencing DSCR8 inhibited Cdc42 expression (Figure 6A). The MTT method, a Transwell assay, and flow cytometry were conducted to confirm whether DSCR8 could affect GC cell proliferation, invasion, the cell cycle, and cell apoptosis by regulating Cdc42. The results demonstrated that silencing DSCR8 significantly decreased GC cell proliferation (Figure 6B) and invasion (Figure 6C) abilities, whereas these abilities were reversed when Cdc42 was overexpressed, suggesting that silencing DSCR8 affected Cdc42 expression and its function in cells. Flow cytometry showed that silencing DSCR8 inhibited the cell cycle progression, showing an increase in the number of cells in the G_0/G_1 phase, and the proportion of cells in the G_0/G_1 phase was significantly recovered when Cdc42 was overexpressed simultaneously (Figure 6D). Additionally, low expression of DSCR8 and Cdc42 promoted cell apoptosis of GC cells (Figure 6E). Collectively, these findings showed that DSCR8 regulates Cdc42 expression by mediating miR-137, ultimately affecting GC cell proliferation, invasion, the cell cycle, and cell apoptosis.

Low expression of DSCR8 inhibits the growth of GC *in vivo*

Finally, a xenograft mouse model was applied to study the effect of DSCR8. It was found that the tumor growth was reduced in the sh-DSCR8 group compared with that in the sh-NC group (Figure 7A). The tumor was weighed after 35 days, and it was found that the tumor weight in the sh-DSCR8 group was only half that in the sh-NC group (Figure 7B). Immunohistochemistry (IHC) and terminal deoxynucleotidyl transferase-mediated nick end labeling (TUNEL) staining illustrated that the percentage of Ki-67-positive cells was significantly decreased in the sh-DSCR8 group (Figure 7C), while the percentage of TUNEL-positive cells was increased (Figure 7D). Moreover, the result of qRT-PCR showed that DSCR8 and Cdc42 were decreased in mouse tumors injected with sh-DSCR8, whereas miR-137 exhibited a higher expression level in the sh-DSCR8 group relative to that in the sh-NC group (Figure 7E). Western blot showed that the protein expression level of Cdc42 was relatively lower in the sh-DSCR8 group than that in the sh-NC group (Figure 7F). Therefore, our study proved that low expression of DSCR8 could reduce the growth of GC cells *in vivo*.

In conclusion, we found that DSCR8 was significantly upregulated in GC, and it positively regulated the expression of Cdc42 by sponging miR-137, thereby promoting the proliferation, invasion, and cell cycle progression of GC cells, and reducing the apoptosis rate (Figure 8).

DISCUSSION

An increasing number of studies have reported that lncRNAs have great potential value in the diagnosis and treatment of GC, such as lncRNA CADM1-AS1,[31] lncRNA p4516,[16] and B3GALT5-AS1.[32] lncRNAs RP11-169F17.1 and RP11-669N7.2 are found to be novel prognostic biomarkers of GC and might play an important role in gastric disorders caused by *Helicobacter pylori* infection, as revealed by the bioinformatics analysis of Yang and Song.[33] Additionally, KRT19P3 was found to inhibit the proliferation and metastasis of GC by COPS7A meditating the nuclear factor κB (NF-κB) pathway.[34] Taken together, these studies indicate that lncRNA is abnormally expressed in the progression of GC, and it promotes the occurrence and development of GC.

Our study explored the mechanism of DSCR8 in GC. We found that DSCR8 was overexpressed in GC tissue and cells, which was in accordance with the results of TCGA data, suggesting that DSCR8 has a great potential to be an oncogene in GC. DSCR8 was previously reported in uterine cancer and melanoma.[18,19] Wang et al.[35] investigated the expression and role of DSCR8 in hepatocellular carcinoma (HCC), and they found that DSCR8 can activate the Wnt/β-catenin signaling pathway to promote the progression of HCC via the DSCR8/miR-485-5p/FZD7 axis. However, the role of DSCR8 in GC has not been elucidated. Hence, DSCR8 was overexpressed or silenced in our study to explore its role in proliferation, invasion, the cell cycle, and cell apoptosis of GC cells. We found that silencing DSCR8 suppressed GC cell proliferation and invasion as well as blocked the cell cycle in the G_0/G_1 phase and facilitated cell apoptosis. Experiments with mice also fully validated that the low expression of DSCR8 inhibited the progression of GC.

Subsequently, we speculated that DSCR8 may act as a molecular sponge of miR-137 by bioinformatics analysis. miR-137 has been reported to serve as a tumor suppressor in various cancers.[30,36,37] In the present study, we found that miR-137 was significantly downregulated in GC and had a negative correlation with DSCR8. FISH experiments also suggested that DSCR8 was located in both the nucleus and cytoplasm, which increased the possibility of DSCR8 sponging miR-137. A dual-luciferase reporter gene assay and RIP experiment confirmed that miR-137 was a direct target of DSCR8. Collectively, these findings elucidate that DSCR8 promotes GC cell proliferation and invasion and inhibits cell apoptosis by downregulating miR-137 expression.

Furthermore, to investigate how miR-137 affects the progression of GC, we combined bioinformatics analysis with previous studies[24,38] and found that Cdc42, which was downregulated by miR-137, was significantly differentially expressed in GC. Numerous studies showed that Cdc42 was highly expressed in

clinical samples). (E) Pearson correlation analysis of DSCR8 and miR-137. (F) Differential expression of miR-137 in different cell lines. (G) miR-137 expression in each treatment group. (H) DSCR8 expression in each treatment group. (I and J) A dual-luciferase reporter gene assay and RIP experiment were conducted to verify the binding relationship between miR-137 and DSCR8. (K) The expression of DSCR8 and miR-137 in biotinylated DSCR8 and negative control (NC) probe pull-down samples were detected by qRT-PCR. n All data are measured data, expressed as mean ± standard deviation. = three independent experiments. *$p < 0.05$.

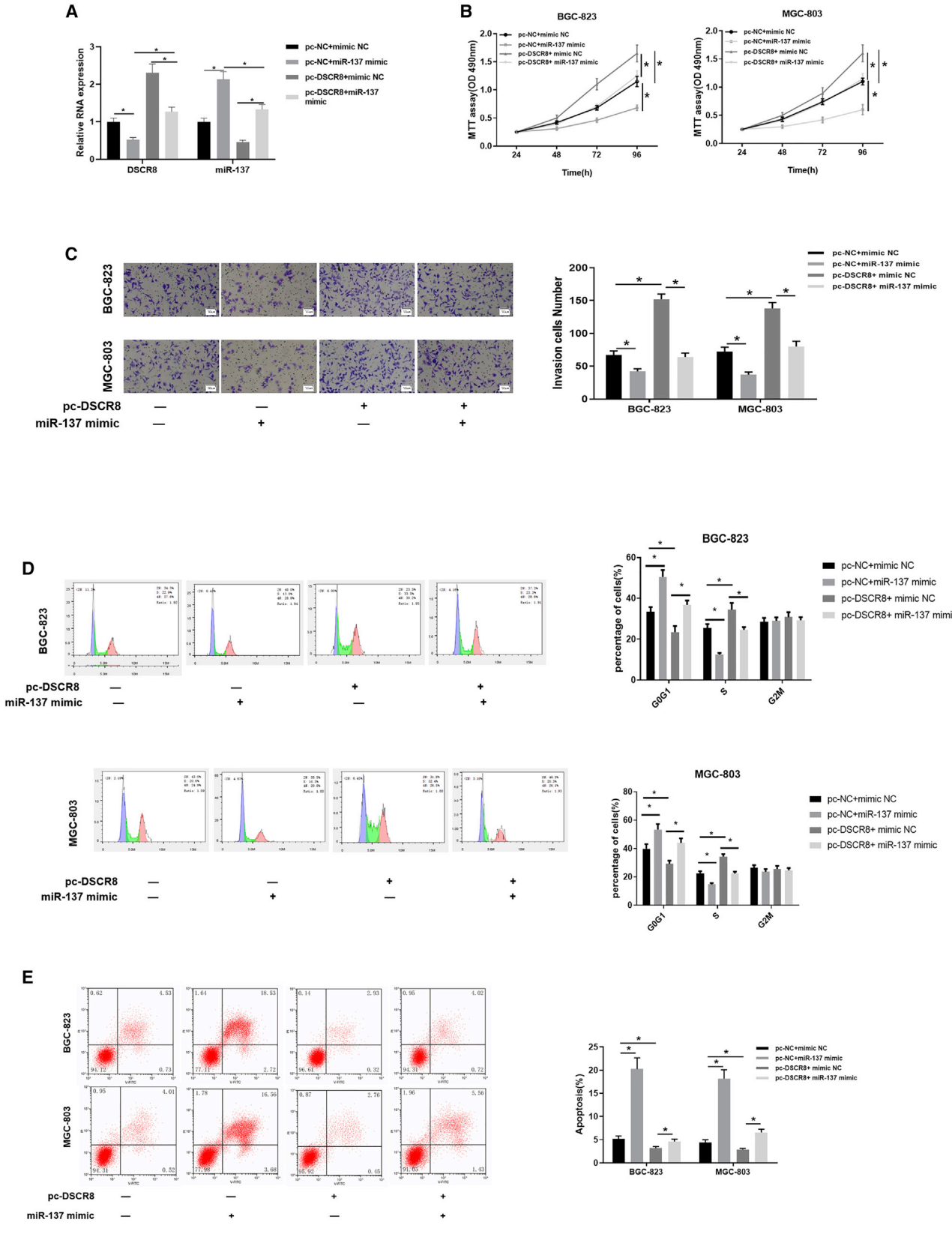

(legend on next page)

GC and promotes GC cell proliferation, migration, invasion, and the cell cycle.[39–41] In our study, Cdc42 was considerably highly expressed in GC tumor samples when compared with adjacent normal samples, which was consistent with the results of bioinformatics analysis and previous studies. A dual-luciferase reporter gene assay suggested that there was a targeted binding relationship between miR-137 and Cdc42. In order to validate the positive correlation between DSCR8 and Cdc42, rescue experiments were designed, which found that silencing DSCR8 decreased Cdc42 expression and inhibited some cell behaviors of GC cells, while the cell apoptosis rate was elevated. However, these functions were obviously reversed when Cdc42 was overexpressed and DSCR8 expression was silenced. Taken together, these findings indicate that DSCR8 expression could affect Cdc42 expression and its biological function on the progression of GC.

Our study first explained the molecular mechanism of lncRNA DSCR8 in the progression of GC by regulating miR-137/Cdc42. The results of our study demonstrated that high expression of DSCR8 resulted in the downregulation of miR-137, whereas low expression of miR-137 reduced its binding with Cdc42, leading to the upregulation of Cdc42, thus promoting GC cell proliferation, invasion, and the cell cycle and reducing cell apoptosis rate. These findings provide a novel direction that the lncRNA DSCR8 can be used for the diagnosis and molecular targeted treatment of GC.

With the development of molecular biotechnology and high-throughput sequencing technology, a large number of studies have confirmed that a variety of lncRNAs are differentially expressed in GC tissue or plasma of GC patients. Their expression levels are also related to the clinicopathological characteristics of GC, which is expected to provide new targets and molecular markers for the diagnosis, treatment, and prognosis of GC.[42–44] However, due to the diversity and uncertainty of lncRNAs, there are still many key problems to be solved in the role and mechanism of lncRNA in GC, including (1) the specific mechanisms of lncRNAs regulating upstream and downstream signaling pathways, (2) the fact that lncRNAs may also be involved as a drug resistance mechanism, (3) the detection of important lncRNAs with low expression levels *in vivo* by current techniques, and (4) the delivery of therapeutic lncRNAs into target tissue and evaluation of their safety. At present, lncRNA studies have not been fully carried out, and there are no approved lncRNA-targeted drugs.[45] A certain period of time is still needed before lncRNA can be transformed from basic research into clinical application. It is of great importance to understand detailed biological functions and mechanisms of lncRNA, which will lay a foundation for the discovery of new disease therapeutic targets and strategies.

MATERIALS AND METHODS

Bioinformatics analysis

STAD gene expression profiles were acquired from TCGA database (https://portal.gdc.cancer.gov/). The ID was converted by a GTF (GRCh38.p5)ftp://ftp.ncbi.nlm.nih.gov/genomes/Homo_sapiens/GFFgenecode database (http://ftp.ebi.ac.uk/pub/databases/gencode/Gencode_human/release_38/gencode.v38.annotation.gtf.gz) annotation file and the lncRNA expression profiles were extracted. The expression profiles included 32 normal samples and 373 GC tissue samples using the R language edgeR package for differential analysis, with normal samples as a control. A |logFC| >2 and an adj. p value <0.05 were lncRNA screening criteria. Similarly, STAD miRNA expression profiles were acquired from TCGA database (https://portal.gdc.cancer.gov/). The expression profiles included 45 normal samples and 444 GC tissue samples using the R language edgeR package for differential analysis, with normal samples as a control. A |logFC| >1.5 and an adj. p value <0.05 were miRNA screening criteria. The target genes and their binding sites of DSCR8 were predicted using miRcode[46] (http://www.mircode.org/), as well as the TargetScan 7.1 database[47] (http://www.targetscan.org) to predict the binding sites of miR-137 and Cdc42.

Sample collection

GC tumor tissue samples and paired adjacent normal tissue samples were collected from 60 cases treated in the Lishui People's Hospital of Zhejiang Province from September 2018 to August 2019. All patients had not received any chemotherapy or radiotherapy prior to surgery. GC tumor tissue and paired adjacent normal tissue obtained from patients were identified by experienced pathologists. Tumor tissue samples were immediately preserved in RNA solution after surgical resection. This study was approved by the Ethic Committee of the Lishui People's Hospital of Zhejiang Province and agreed to by all of the patients. The pathological data, including age, sex, tumor size, and disease stage, are shown in Table 1. The samples were divided into a high-expression group and a low-expression group according to the median DSCR8 expression in all tumor samples.

Cell lines and cell culture

The human GC cell lines BGC-823 (BNCC100086), MGC-803 (BNCC340396), HGC-27 (BNCC100097), and AGS (BNCC102154) and the human normal stomach cell line GES-1 (BNCC342032) were all purchased from BeNa Culture Collection (China). All cell lines were grown in Roswell Park Memorial Institute (RPMI) 1640 medium (Gibco; Thermo Fisher Scientific, Waltham, MA, USA) supplemented with 10% fetal bovine serum (FBS; HyClone; GE Healthcare Life Sciences, Logan, UT, USA), 100 U/mL streptomycin (Gibco; Thermo Fisher Scientific), and 100 U/mL penicillin (Gibco; Thermo Fisher Scientific) and maintained in a thermostatic incubator with 5% CO_2 at 37°C before use. The media were replaced at an interval of

Figure 4. The function of DSCR8 is mediated by miR-137

(A) DSCR8 and miR-137 expression levels, (B) cell proliferation activity, (C) cell invasion ability (100×), (D) cell cycle status, and (E) apoptosis in each transfection group (pc-NC+mimic NC, pc-NC+miR-137 mimic, pc-DSCR8+mimic NC, pc-DSCR8+miR-137 mimic) of GC cell lines BGC-823 and MGC-803. n = three independent experiments. All data are measured data, expressed as mean ± standard deviation. *p < 0.05.

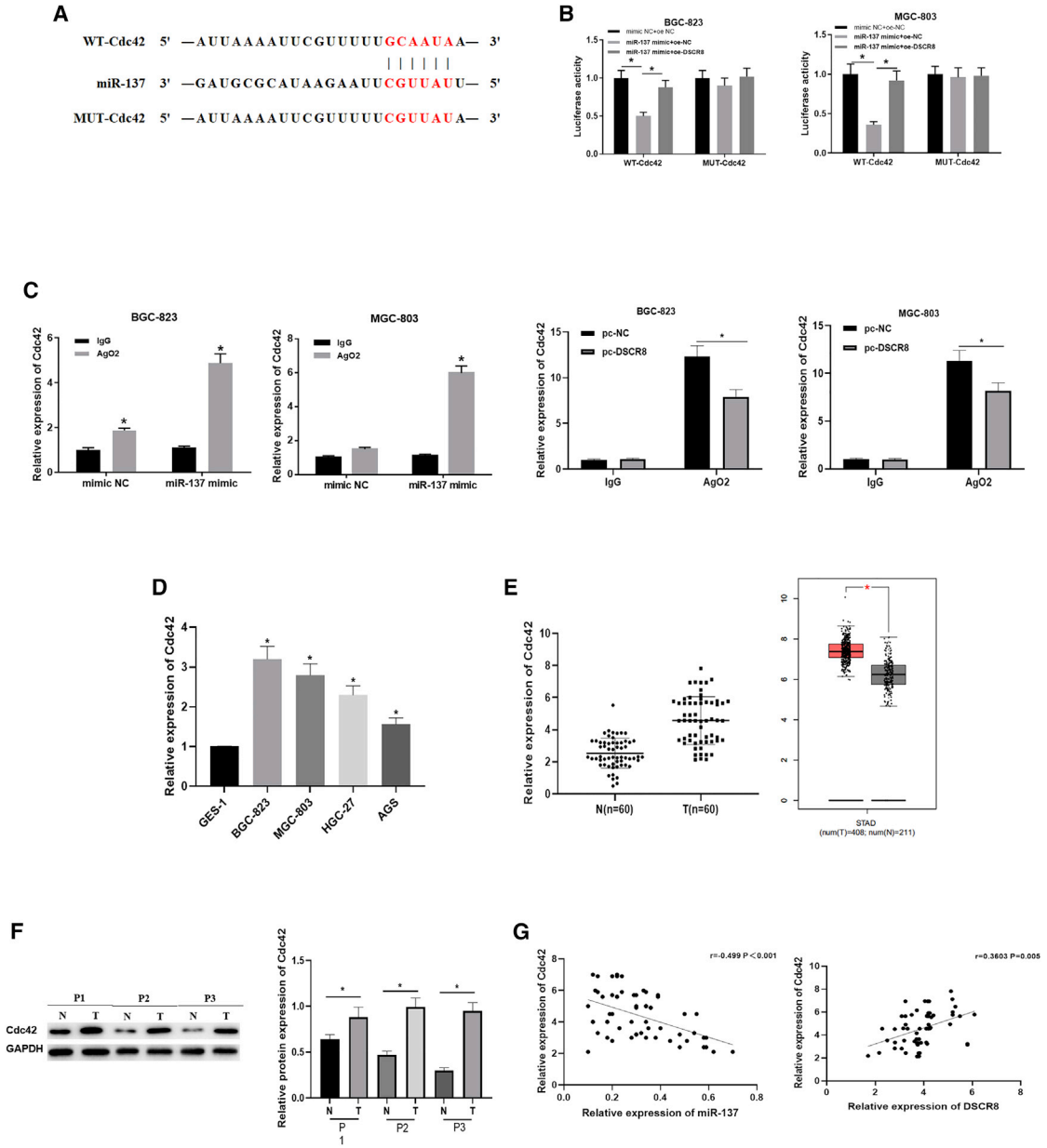

Figure 5. Cdc42 is highly expressed in GC tissue and is negatively regulated by miR-137

(A) The targeted binding sites of miR-137 on the Cdc42 3′ UTR. (B) A dual-luciferase reporter gene and (C) RIP experiment were used to verify the targeted binding relationship between miR-137 and Cdc42. (D) Expression level of CDC42 in human gastric mucosa cells (GES-1) and GC cell lines. (E) Expression of Cdc42 in clinical tissue samples (left, normal, n = 60; right, tumor, n = 60) as well as in TCGA-STAD and GTEx databases (left, tumor, n = 408; right, normal, n = 211). (F) Differential expression of CDC42 in clinical tissue of GC (P1, P2, and P3 represent clinical samples of GC patients). (G) Pearson correlation analysis of miR-137 and Cdc42 (left), as well as DSCR8 and Cdc42 (right). n = three independent experiments. All data are measured data, expressed as mean ± standard deviation. *p < 0.05.

2–3 days. The cells of two to four generations after resuscitation were used in this study.

Cell transfection

The sh-NC and sh-DSCR8, pc-NC, and pc-DSCR8 (DSCR8 overexpression vector) lentiviral packaged vectors purchased from Invitrogen (Carlsbad, CA, USA) were used to establish GC cell lines with stable expression. The mimic NC and miR-137 mimic, oe-NC, and oe-Cdc42 accessed from GenePharma (Shanghai, China) were transiently transfected into GC cell lines by Lipofectamine 2000 (Thermo Fisher Scientific) according to the manufacturer's instructions. Thereafter, the transfected cells were cultured in media with 5% CO_2 at

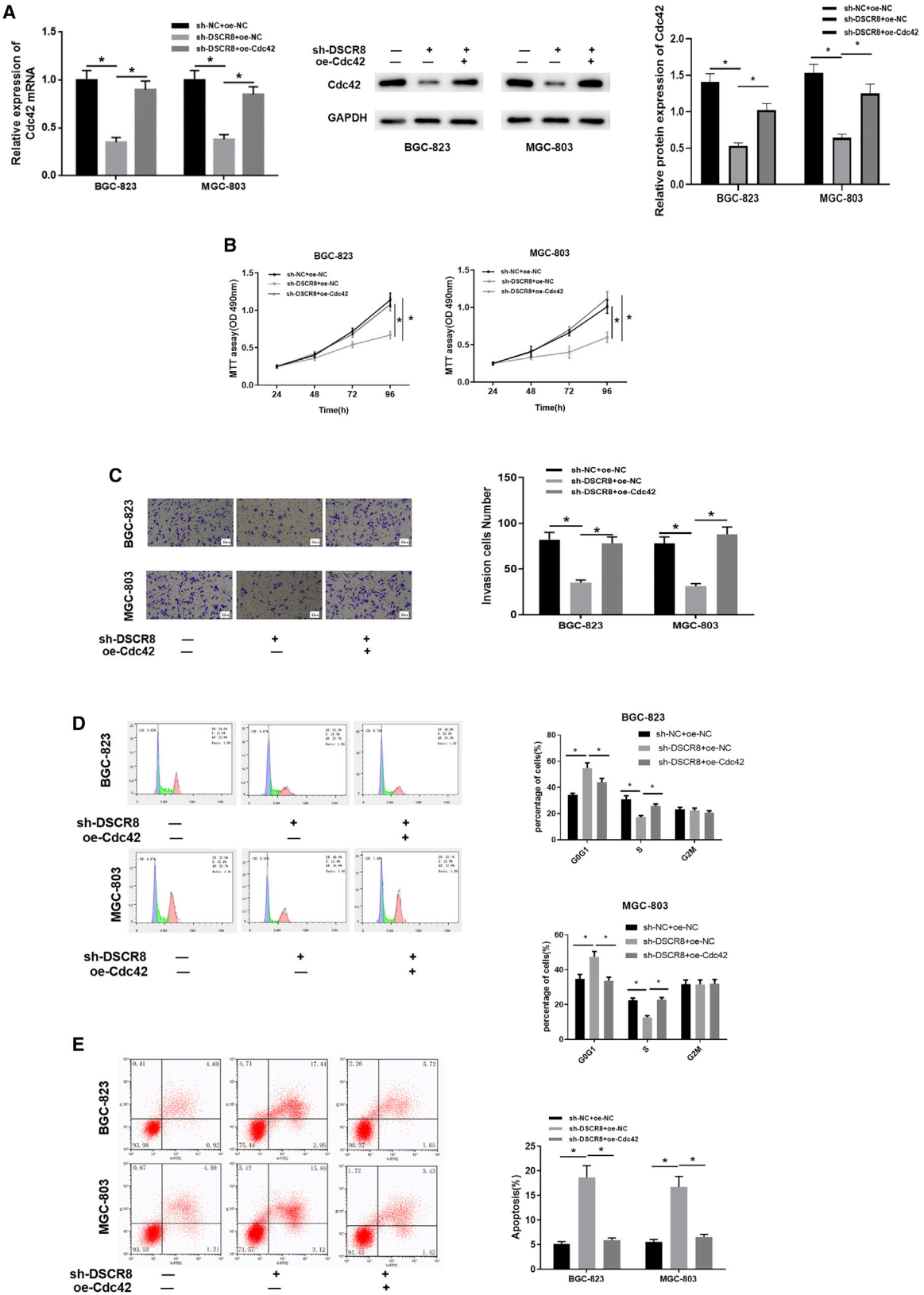

(legend on next page)

37°C before use. All cells were incubated in complete medium for at least 24 h before transfection and washed with phosphate-buffered saline (PBS, pH 7.4) before transient transfection.

RNA extraction and qRT-PCR

Total RNA was isolated from tissue and cells by TRIzol reagent (Invitrogen) according to manufacturer's protocols. miRNA was reversely transcribed into cDNA by a TransScript miRNA first-strand cDNA synthesis SuperMix kit (AT351-01; TransGen Biotech, Beijing), while lncRNA and mRNA were reversely transcribed into cDNA by a TransScript one-step gDNA removal and cDNA synthesis SuperMix kit (AT311-02; TransGen Biotech, Beijing). SYBR Premix Ex Taq (TaKaRa, Otsu, Shiga, Japan) was applied for qRT-PCR, and an Applied Biosystems 7300 real-time PCR system (Applied Biosystems, USA) was used to detect the expression levels of DSCR8, miR-137, and Cdc42. Primer sequences for qRT-PCR (as shown in Table 2) were purchased from Sangon (Shanghai, China). GAPDH was taken as an internal reference for DSCR8 and Cdc42, while U6 was taken as an internal reference for miR-137. The relative expression of target genes in the control group and test group were compared and analyzed by the $2^{-\Delta\Delta Ct}$ method.

Western blot

After being transfected for 48 h, cells in different groups were washed with cold PBS three times and lysed on ice with whole-cell lysate for 10 min, and then the protein concentration was determined using a bicinchoninic acid (BCA) kit (Thermo Fisher Scientific, Waltham, MA, USA). Next, 30 μg of total protein samples was treated by sodium dodecyl sulfate-polyacrylamide gel electrophoresis (SDS-PAGE) and transferred onto polyvinylidene fluoride (PVDF) membranes (Amersham, USA). After being blocked with 5% skim milk at room temperature for 1 h, the blocking buffer was discarded and the membranes were incubated with Cdc42 rabbit polyclonal antibody (Abcam, Cambridge, UK) and GAPDH rabbit polyclonal antibody (Abcam, Cambridge, UK) overnight at 4°C. PBS + 0.1% Tween 20 (PBST) was used to wash the membranes three times, 10 min for each time. Horseradish peroxidase-labeled secondary antibody goat anti-rabbit immunoglobulin G (IgG) H&L (HRP) (Abcam, Cambridge, UK) was added to the membranes for 1 h of incubation at room temperature, and then the membranes were washed with PBST for 10 min three times. All protein bands were visualized under an optical luminometer (GE Healthcare, USA) and then imaged.

MTT assay

The MTT assay method (Sigma-Aldrich) was applied to examine GC cell proliferation in different groups. Transfected cells were seeded into 96-well plates at a density of 2×10^3 cells/well. Then, 20 μL of MTT (0.5 mg/mL; Sigma-Aldrich, St. Louis, MO, USA) was added to each well at 24, 48, 72, and 96 h, respectively. The incubation was terminated after cells were cultured at the indicated time points for a further 4 h at 37°C, and the supernatant in each well was removed. Afterward, 150 μL of dimethyl sulfoxide (DMSO; Sigma-Aldrich) was added to each well for 20 min to fully dissolve the crystal substance. The optical density (OD) value at 490 nm was recorded.

Transwell invasion assay

GC cells (approximately 5×10^4) were placed into the upper chamber of 24-well Transwell chambers, which were coated with 500 ng/mL Matrigel matrix (Corning Life Sciences, NY). RPMI 1640 medium supplemented with 10% FBS was added to the lower chamber. Cells were then nurtured in an incubator with 5% CO_2 at 37°C, and the Transwell inserts were removed after 36 h of incubation. For the cells invading the lower chambers, 4% paraformaldehyde was used for 30 min of fixation, and 0.1% crystal violet was used for staining. Five fields were randomly selected to calculate the invading cells. The experiment was repeated three times.

Cell cycle

For cell cycle analysis, transfected cells were seeded into 6-cm culture dishes with a density of 2×10^5 cells per dish. Transfected cells were digested by trypsin K when cells grew to 80% in confluence, and then washed with cold PBS to collect a single-cell suspension. After being fixed with 75% ethanol, the cells were treated by RNase A (Sigma-Aldrich) and then stained with 500 μL of propidium iodide (PI; Sigma-Aldrich). Flow cytometry (Beckman Coulter) was used for analyzing cell cycle distribution, and the percentages of cells in the G_0/G_1 phase, S phase, and G_2/M phase were calculated and compared.

Cell apoptosis

An annexin V/PI apoptosis detection kit (Bender MedSystems, Austria) was applied for detecting cell apoptosis according to the manufacturer's instructions. Next, 5×10^5 cells were suspended in 500 μL (1×) of binding buffer (10 mM HEPES [pH 7.4], 140 mM NaCl, 2.5 mM $CaCl_2$). Annexin V (1:20) was used to culture cells for 5 min, and then PI (1 mg/mL) was added for 15 min of incubation. Flow cytometry was used for the assessment of cell apoptosis rate.

Dual-luciferase reporter gene assay

A dual-luciferase reporter gene assay was conducted to verify the targeted binding relationship between DSCR8 and miR-137, or miR-137 and Cdc42. Sequences of the 3′ UTR of DSCR8 and Cdc42 amplified by PCR were inserted downstream of the luciferase vector pmirGLO (Promega, WI, USA) to establish WT-DSCR8 and WT-Cdc42 constructs. Mutation sites at the 3′ UTR of DSCR8 and Cdc42 were generated using the QuickChange multi site-directed mutagenesis

Figure 6. DSCR8 promotes GC cell processes by regulating Cdc42

(A) mRNA and protein expression levels of Cdc42 in different transfection groups (sh-NC+oe-NC, sh-DSCR8+oe-NC, sh-DSCR8+oe-CDC42). (B) Cell proliferation ability of BGC-823 and MGC-803 cells in each transfection group. (C) Cell invasion ability of BGC-823 and MGC-803 cells in each transfection group (100×). (D) Cell cycle of BGC-823 and MGC-803 cells in each transfection group. (E) Cell apoptosis of BGC-823 and MGC-803 cells in each transfection group. n = three independent experiments. All data are measured data, expressed as mean ± standard deviation. *$p < 0.05$.

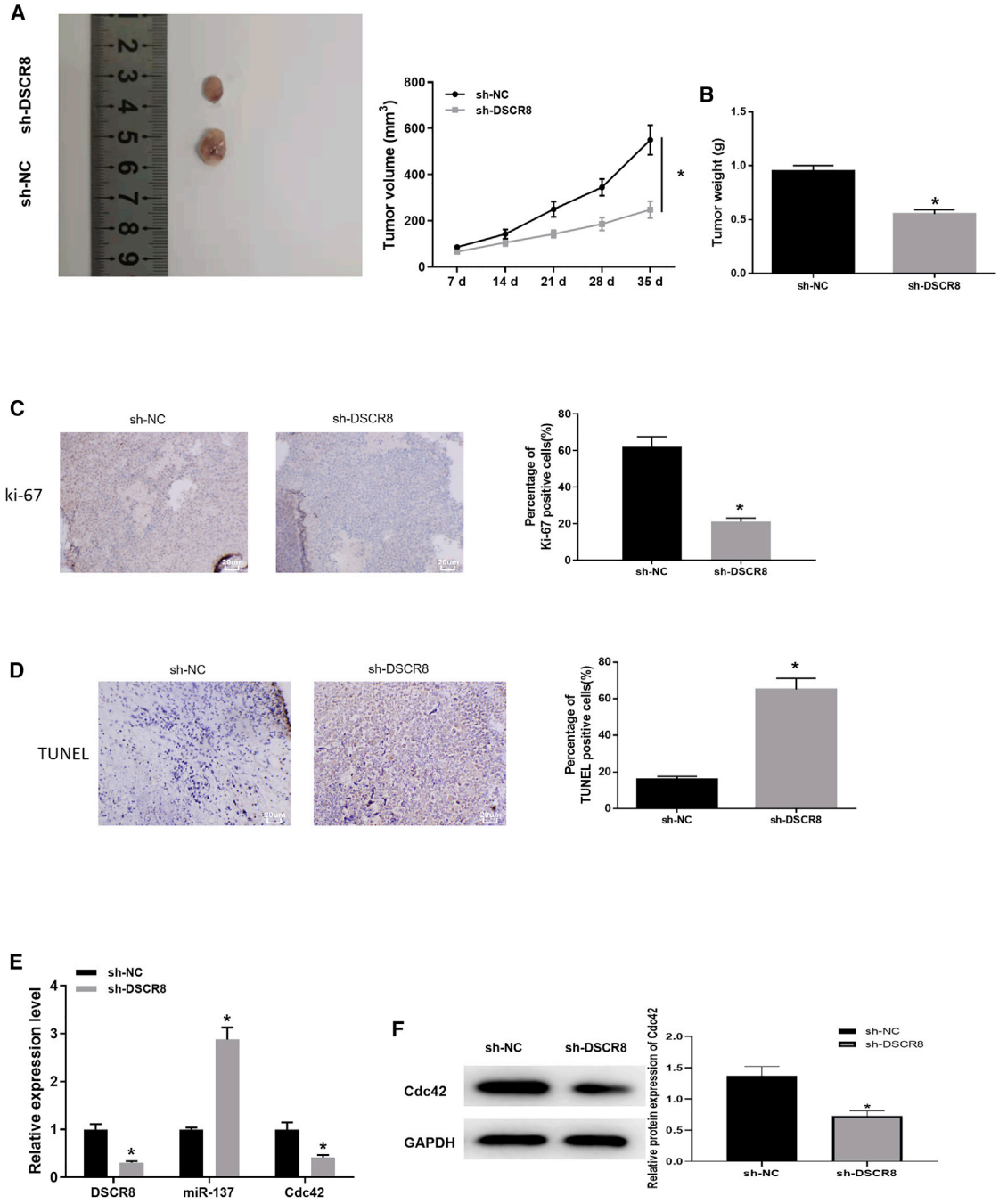

Figure 7. Low expression of DSCR8 inhibits cell growth of GC *in vivo*

(A) Tumor size and tumor volume (n = 5 per group). (B) Tumor weight after 35 days. (C) Ki-67-positive cells and (D) cell apoptosis in xenograft tumor mouse models, respectively (original magnification, ×400; scale bars, 20 μm). (E) RNA expression levels of DSCR8, miR-137, and Cdc42 in tumor tissue. (F) Protein expression level of Cdc42 in tumor tissue. n = three independent experiments. All data are measured data, expressed as mean ± standard deviation. *$p < 0.05$.

kit (Stratagene, La Jolla, CA, USA), and mutant (MUT)-DSCR8 and MUT-Cdc42 constructs were then built. Subsequently, these vectors were co-transfected with miR-137 mimic/mimic NC into BGC-823 and MGC-803 cells. Renilla luciferase expression vector pRL-TK (TaKaRa, Dalian, China) was taken as an internal reference. The activity of luciferase was assayed by a Dual-Luciferase assay kit (Promega, Madison, WI, USA) after 48 h of incubation. The experiment was conducted in triplicate.

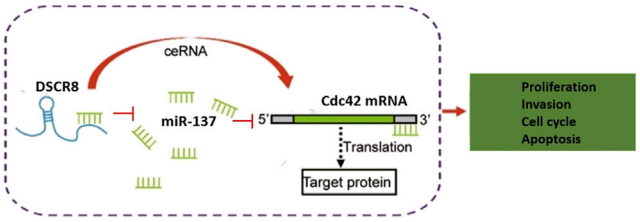

Figure 8. The regulatory mechanism of DSCR8 in the pathogenesis of GC
DSCR8 can adsorb miR-137 to weaken its inhibitory effect on Cdc42 expression, thus promoting the proliferation, invasion, and cell cycle progression of GC cells, and reducing the apoptosis rate of GC cells.

RIP assay

A RIP assay was performed by a Magna RIP RNA-binding protein immunoprecipitation kit (Millipore, USA) in line with protocols. First, GC cells were harvested and lysed in RIP lysis buffer for 30 min. Then, the cell extraction was incubated with RIP buffer containing magnetic beads, followed by incubation with Ago2 rabbit polyclonal antibody (Abcam, Cambridge, UK) with the ordinary rabbit IgG (Abcam, Cambridge, UK) as the NC. The samples digested with Proteinase K were purified and then RNA was extracted for further qRT-PCR analysis.

Biotin pull-down assay

BGC-823 and MGC-803 cells were transfected with biotin-labeled WT-miR-137, MUT-miR-137, and NC (Guangzhou RiboBio). According to the manufacturer's protocol, cell lysate was collected 48 h after transfection and incubated with Dynabeads M-280 streptavidin (Invitrogen, CA, USA) at 4°C for 3 h. Then, the lysate was washed with ice-cold lysis buffer three times and high-salt buffer solution (0.1% SDS, 1% Triton X-100, 2 mM EDTA, 20 mM Tris-HCl [pH 8.0], and 500 mM NaCl) once.[48] Bound RNA was purified with TRIzol and analyzed by qRT-PCR.

FISH

Fluorescence-labeled probes for lncRNA DSCR8 were accessed from NatureGene (Beijing, China). After being thawed at room temperature, the cells were digested with Proteinase K and denatured by methanamide and then hybridized with the DSCR8 probe at 42°C. Then, the nuclei were counterstained by 4′,6-diamino-2-phenylindole (DAPI). A drop of fixed medium of fluorescence decay was added to the samples and analyzed under a fluorescence microscope. The excitation wavelength used in DAPI was 360 nm, while that used in DSCR8 was 490 nm.

IHC and TUNEL staining

Paraffin-embedded GC tissue sections used for the detection of Cdc42 expression were conventionally dehydrated, washed with distilled water three times, and incubated with 3% hydrogen peroxide for 10 min. After being rinsed in PBS, the sections were blocked with 10% goat serum for 30 min. Thereafter, the sections were incubated with rabbit antibody anti-Ki-67 (Abcam, Cambridge, UK) at 4°C overnight, followed by secondary antibody goat anti-rabbit IgG H&L (HRP) (Abcam, Cambridge, UK) for 60 min at 37°C. Then, the sections were developed with diaminobenzidine (DAB) solution, while hematoxylin was used for counterstaining. Additionally, an *in situ* cell death detection kit (Roche, Basel, Switzerland) was used for TUNEL staining, and the result was observed under an optical microscope (×400) (Olympus).

Table 2. Primer sequence for qRT-PCR

Target gene	Primer (5′-3′)
DSCR8	F: GTGCAGTGGTTCAATCACGGA
	R: CCAGCACTTTCGGTCTTGG
miR-137	F: TATTGCTTAAGAATACGCGTAG
	R: AACTCCAGCAGGACCATGTGAT
Cdc42	F: CCATCGGAATATGTACCGACTG
	R: CTCAGCGGTCGTAATCTGTCA
U6	F: CTCGCTTCGGCAGCACA
	R: AACGCTTCACGAATTTGCGT
GAPDH	F: GGAGCGAGATCCCTCCAAAAT
	R: GGCTGTTGTCATACTTCTCATGG

In vivo experiments on mice

A total of 10 BALB/c male athymic mice (4 weeks of age) were purchased from Shanghai SLAC Laboratory Animal Co. (Shanghai, China) and then divided into two groups (five in each group). The GC cell line BGC-823 transfected with sh-NC or sh-DSCR8 was subcutaneously injected into the left lower limb of mice according to previous studies. Tumor size was measured using a caliper every 7 days, and tumor volume was calculated using the following formula: volume (cm^3) = (length × width2)/2. After 35 days, the mice were euthanized and tumor weight was measured. Experiments were performed under a project license granted by the institutional ethics committee board of the Lishui People's Hospital of Zhejiang Province in compliance with the Lishui People's Hospital of Zhejiang Province institutional guidelines for the care and use of animals.

Data analysis

All data were processed by SPSS 22.0 software (SPSS, Chicago, IL, USA) and GraphPad Prism 6.0 software (GraphPad, San Diego, CA, USA). Measurement data are presented by means ± standard deviation. Subsequently, a t test was applied for comparison between two groups, while a one-way analysis of variance (ANOVA) was performed for comparisons among more than two groups. $p < 0.05$ was considered statistically significant.

Data availability

The data used to support the findings of this study are included within the article. The data and materials in the current study are available from the corresponding author on reasonable request.

AUTHOR CONTRIBUTIONS

Z.C. contributed to the study design. C.X. conducted the literature search. X.P. acquired the data. G.C. and Z.C. wrote the manuscript.

M.L. performed data analysis and drafted the manuscript. J.L. and Z.C. revised the manuscript. Y.M. and Z.C. gave the final approval of the version to be submitted.

DECLARATION OF INTERESTS

The authors declare no competing interests.

REFERENCES

1. Zhang, G., Li, S., Lu, J., Ge, Y., Wang, Q., Ma, G., Zhao, Q., Wu, D., Gong, W., Du, M., et al. (2018). lncRNA MT1JP functions as a ceRNA in regulating FBXW7 through competitively binding to miR-92a-3p in gastric cancer. Mol. Cancer *17*, 87.
2. Wang, Q., Shang, J., Wang, X., Ziang, L., Cheng, J., and Lin, J. (2021). New advances in molecular targeted drug therapy and immunotherapy for advanced gastric carcinoma. Wuhan Daxue Xuebao Yixue Ban *42*, 407–412.
3. Orditura, M., Galizia, G., Sforza, V., Gambardella, V., Fabozzi, A., Laterza, M.M., Andreozzi, F., Ventriglia, J., Savastano, B., Mabilia, A., et al. (2014). Treatment of gastric cancer. World J. Gastroenterol *20*, 1635–1649.
4. Matuschek, C., Haussmann, J., Bölke, E., Tamaskovics, B., Djiepmo Njanang, F.J., Orth, K., Peiper, M., Gerber, P.A., Anooshar, B., Kammers, K., and Budach, W. (2019). Adjuvant radiochemotherapy vs. chemotherapy alone in gastric cancer: a meta-analysis. Strahlenther. Onkol. *195*, 695–706.
5. Johnston, F.M., and Beckman, M. (2019). Updates on management of gastric cancer. Curr. Oncol. Rep *21*, 67.
6. Fu, T., and Song, K. (2016). Research progress of molecular targeted antitumor drugs. J. Pharm. Res. *35*, 412–415.
7. Khalil, A.M., Guttman, M., Huarte, M., Garber, M., Raj, A., Rivea Morales, D., Thomas, K., Presser, A., Bernstein, B.E., van Oudenaarden, A., et al. (2009). Many human large intergenic noncoding RNAs associate with chromatin-modifying complexes and affect gene expression. Proc. Natl. Acad. Sci. USA *106*, 11667–11672.
8. Xue, X., Yang, Y.A., Zhang, A., Fong, K.W., Kim, J., Song, B., Li, S., Zhao, J.C., and Yu, J. (2016). lncRNA HOTAIR enhances ER signaling and confers tamoxifen resistance in breast cancer. Oncogene *35*, 2746–2755.
9. Lee, J.T. (2012). Epigenetic regulation by long noncoding RNAs. Science *338*, 1435–1439.
10. Chery, J. (2016). RNA therapeutics: RNAi and antisense mechanisms and clinical applications. Postdoc J *4*, 35–50.
11. Batista, P.J., and Chang, H.Y. (2013). Long noncoding RNAs: Cellular address codes in development and disease. Cell *152*, 1298–1307.
12. St Laurent, G., Wahlestedt, C., and Kapranov, P. (2015). The landscape of long noncoding RNA classification. Trends Genet. *31*, 239–251.
13. Choudhari, R., Sedano, M.J., Harrison, A.L., Subramani, R., Lin, K.Y., Ramos, E.I., Lakshmanaswamy, R., and Gadad, S.S. (2020). Long noncoding RNAs in cancer: From discovery to therapeutic targets. Adv. Clin. Chem *95*, 105–147.
14. Salmena, L., Poliseno, L., Tay, Y., Kats, L., and Pandolfi, P.P. (2011). A ceRNA hypothesis: The Rosetta Stone of a hidden RNA language? Cell *146*, 353–358.
15. Wei, G.H., and Wang, X. (2017). lncRNA MEG3 inhibit proliferation and metastasis of gastric cancer via p53 signaling pathway. Eur. Rev. Med. Pharmacol. Sci. *21*, 3850–3856.
16. Nie, M.L., Han, J., Huang, H.C., Guo, T., Huangfu, L.T., Cheng, X.J., Li, X.M., Du, H., Li, Q.D., Wen, X.Z., and Ji, J.F. (2019). The novel lncRNA p4516 acts as a prognostic biomarker promoting gastric cancer cell proliferation and metastasis. Cancer Manag. Res. *11*, 5375–5391.
17. Tao, W., Li, Y., Zhu, M., Li, C., and Li, P. (2019). lncRNA NORAD promotes proliferation and inhibits apoptosis of gastric cancer by regulating miR-214/Akt/mTOR axis. Onco Targets Ther *12*, 8841–8851.
18. de Wit, N.J., Weidle, U.H., Ruiter, D.J., and van Muijen, G.N. (2002). Expression profiling of MMA-1a and splice variant MMA-1b: New cancer/testis antigens identified in human melanoma. Int. J. Cancer *98*, 547–553.
19. Risinger, J.I., Chandramouli, G.V., Maxwell, G.L., Custer, M., Pack, S., Loukinov, D., Aprelikova, O., Litzi, T., Schrump, D.S., Murphy, S.K., et al. (2007). Global expression analysis of cancer/testis genes in uterine cancers reveals a high incidence of BORIS expression. Clin. Cancer Res. *13*, 1713–1719.
20. Chen, R., Zhang, Y., Zhang, C., Wu, H., and Yang, S. (2017). miR-137 inhibits the proliferation of human non-small cell lung cancer cells by targeting SRC3. Oncol. Lett. *13*, 3905–3911.
21. Liu, X., Chen, L., Tian, X.D., and Zhang, T. (2017). miR-137 and its target TGFA modulate cell growth and tumorigenesis of non-small cell lung cancer. Eur. Rev. Med. Pharmacol. Sci. *21*, 511–517.
22. He, Z., Guo, X., Tian, S., Zhu, C., Chen, S., Yu, C., Jiang, J., and Sun, C. (2019). MicroRNA-137 reduces stemness features of pancreatic cancer cells by targeting KLF12. J. Exp. Clin. Cancer Res. *38*, 126.
23. Guan, Y., Guan, X., An, H., Baihetiya, A., Wang, W., Shao, W., Yang, H., and Wang, Y. (2019). Epigenetic silencing of miR-137 induces resistance to bicalutamide by targeting TRIM24 in prostate cancer cells. Am. J. Transl. Res. *11*, 3226–3237.
24. Chen, Q., Chen, X., Zhang, M., Fan, Q., Luo, S., and Cao, X. (2011). miR-137 is frequently down-regulated in gastric cancer and is a negative regulator of Cdc42. Dig. Dis. Sci *56*, 2009–2016.
25. Horita, K., Kurosaki, H., Nakatake, M., Ito, M., Kono, H., and Nakamura, T. (2019). Long noncoding RNA UCA1 enhances sensitivity to oncolytic vaccinia virus by sponging miR-18a/miR-182 and modulating the Cdc42/filopodia axis in colorectal cancer. Biochem. Biophys. Res. Commun. *516*, 831–838.
26. Zhu, X., Li, Y., Shen, H., Li, H., Long, L., Hui, L., and Xu, W. (2013). miR-137 inhibits the proliferation of lung cancer cells by targeting Cdc42 and Cdk6. FEBS Lett *587*, 73–81.
27. Wang, Y., Sun, L., Wang, L., Liu, Z., Li, Q., Yao, B., Wang, C., Chen, T., Tu, K., and Liu, Q. (2018). Long non-coding RNA DSCR8 acts as a molecular sponge for miR-485-5p to activate Wnt/β-catenin signal pathway in hepatocellular carcinoma. Cell Death Dis *9*, 851.
28. Dong, L., Cao, X., Luo, Y., Zhang, G., and Zhang, D. (2020). A positive feedback loop of lncRNA DSCR8/miR-98-5p/STAT3/HIF-1α plays a role in the progression of ovarian cancer. Front. Oncol *10*, 1713.
29. Du, Y., Chen, Y., Wang, F., and Gu, L. (2016). miR-137 plays tumor suppressor roles in gastric cancer cell lines by targeting KLF12 and MYO1C. Tumour Biol. *37*, 13557–13569.
30. Liu, M., Lang, N., Qiu, M., Xu, F., Li, Q., Tang, Q., Chen, J., Chen, X., Zhang, S., Liu, Z., et al. (2011). miR-137 targets Cdc42 expression, induces cell cycle G1 arrest and inhibits invasion in colorectal cancer cells. Int. J. Cancer *128*, 1269–1279.
31. Shi, X.Y., Sun, Y.Z., Li, M., and Li, H.Y. (2019). lncRNA CADM1-AS1 serves as a new prognostic biomarker for gastric cancer. Eur. Rev. Med. Pharmacol. Sci. *23* (3, Suppl), 232–238.
32. Feng, W., Zong, W., Li, Y., Shen, X., Cui, X., and Ju, S. (2020). Abnormally expressed long noncoding RNA B3GALT5-AS1 may serve as a biomarker for the diagnostic and prognostic of gastric cancer. J. Cell. Biochem. *121*, 557–565.
33. Yang, J., and Song, H. (2019). Identification of long noncoding RNA RP11-169F17.1 and RP11-669N7.2 as novel prognostic biomarkers of stomach adenocarcinoma based on integrated bioinformatics analysis. Epigenomics *11*, 1307–1321.
34. Zheng, J., Zhang, H., Ma, R., Liu, H., and Gao, P. (2019). Long non-coding RNA KRT19P3 suppresses proliferation and metastasis through COPS7A-mediated NF-κB pathway in gastric cancer. Oncogene *38*, 7073–7088.
35. Wang, Y., Sun, L., Wang, L., Liu, Z., Li, Q., Yao, B., Wang, C., Chen, T., Tu, K., and Liu, Q. (2018). Long non-coding RNA DSCR8 acts as a molecular sponge for miR-485-5p to activate Wnt/β-catenin signal pathway in hepatocellular carcinoma. Cell Death Dis. *9*, 851.
36. Liu, X., Cui, L., and Hua, D. (2018). Long noncoding RNA XIST regulates miR-137-EZH2 axis to promote tumor metastasis in colorectal cancer. Oncol. Res. *27*, 99–106.
37. Wang, Z., Yuan, J., Li, L., Yang, Y., Xu, X., and Wang, Y. (2017). Long non-coding RNA XIST exerts oncogenic functions in human glioma by targeting miR-137. Am. J. Transl. Res. *9*, 1845–1855.
38. Gao, M., Liu, L., Li, S., Zhang, X., Chang, Z., and Zhang, M. (2015). Inhibition of cell proliferation and metastasis of human hepatocellular carcinoma by miR-137 is regulated by CDC42. Oncol. Rep. *34*, 2523–2532.

39. Min, P., Zhao, S., Liu, L., Zhang, Y., Ma, Y., Zhao, X., Wang, Y., Song, Y., Zhu, C., Jiang, H., et al. (2019). MICAL-L2 potentiates Cdc42-dependent EGFR stability and promotes gastric cancer cell migration. J. Cell. Mol. Med. *23*, 4475–4488.

40. Aguilar, B.J., Zhao, Y., Zhou, H., Huo, S., Chen, Y.H., and Lu, Q. (2019). Inhibition of Cdc42-intersectin interaction by small molecule ZCL367 impedes cancer cell cycle progression, proliferation, migration, and tumor growth. Cancer Biol. Ther. *20*, 740–749.

41. Vestre, K., Kjos, I., Guadagno, N.A., Borg Distefano, M., Kohler, F., Fenaroli, F., Bakke, O., and Progida, C. (2019). Rab6 regulates cell migration and invasion by recruiting Cdc42 and modulating its activity. Cell. Mol. Life Sci. *76*, 2593–2614.

42. Zhang, G., Chi, N., Lu, Q., Zhu, D., and Zhuang, Y. (2020). lncRNA PTCSC3 Is a biomarker for the treatment and prognosis of gastric cancer. Cancer Biother. Radiopharm *35*, 77–81.

43. Huang, S., and Chen, L. (2019). Overexpression of lncRNA LINC01793 acts as a potential predictor for progression and poor prognosis of gastric cancer. Histol. Histopathol *34*, 233–239.

44. Zhuo, W., Liu, Y., Li, S., Guo, D., Sun, Q., Jin, J., Rao, X., Li, M., Sun, M., Jiang, M., et al. (2019). Long noncoding RNA GMAN, up-regulated in gastric cancer tissues, is associated with metastasis in patients and promotes translation of ephrin A1 by competitively binding GMAN-AS. Gastroenterology *156*, 676–691.e11.

45. Blokhin, I., Khorkova, O., Hsiao, J., and Wahlestedt, C. (2018). Developments in lncRNA drug discovery: Where are we heading? Expert Opin. Drug Disc *13*, 837–849.

46. Jeggari, A., Marks, D.S., and Larsson, E. (2012). miRcode: A map of putative microRNA target sites in the long non-coding transcriptome. Bioinformatics *28*, 2062–2063.

47. Riffo-Campos, Á.L., Riquelme, I., and Brebi-Mieville, P. (2016). Tools for sequence-based miRNA target prediction: What to choose? Int. J. Mol. Sci *17*, 1987.

48. Wang, S.H., Zhang, W.J., Wu, X.C., Weng, M.Z., Zhang, M.D., Cai, Q., Zhou, D., Wang, J.D., and Quan, Z.W. (2016). The lncRNA MALAT1 functions as a competing endogenous RNA to regulate MCL-1 expression by sponging miR-363-3p in gallbladder cancer. J. Cell. Mol. Med *20*, 2299–2308.